ZEAXANTHIN ([3R,3'R]-β,β-CAROTENE-3-3'DIOL) AS A RESONANCE RAMAN AND VISIBLE ABSORPTION PROBE OF MEMBRANE STRUCTURE

R. MENDELSOHN AND R. W. VAN HOLTEN, *Department of Chemistry, Olson Laboratories, Rutgers University, Newark, New Jersey 07102 U.S.A.*

ABSTRACT When zeaxanthin ([3R,3R']-β,β-carotene-3,3'diol) is inserted into phospholipid dispersions and the latter heated through their gel-liquid crystal phase transitions, large changes are noted in the resonance Raman and absorption spectra of the carotenoid molecule. By analogy with the data of Carey and co-workers (*J. Raman Spectrosc.* **6**:282) who studied the aggregation of zeaxanthin in acetone-water solutions, it is suggested that the carotenoid aggregates in the phospholipid gel state while forming a monomer in liquid crystal phases. The alterations in both the visible absorption and resonance Raman data have been used to monitor phospholipid phase behavior in dipalmitoylphosphatidylcholine and distearoylphosphatidylcholine, (DSPC) one-component systems and binary mixtures. The phase diagram obtained for the binary system, as constructed from visible absorption and resonance Raman data, is compared with that of Shimshick and McConnell (*Biochemistry.* **12**:2351) obtained from electron spin resonance (ESR) studies. Although the agreement between absorption and ESR data is generally satisfactory, onset temperatures for phase separation at low DSPC mole fractions deduced from resonance Raman measurements are several degrees lower than those from the other methods. Nevertheless, the use of zeaxanthin as a resonance Raman and visible absorption probe behavior will be useful in some situations where ordinary Raman spectroscopic data cannot be obtained easily. The advantage of the resonance Raman approach is illustrated in a study of the phase behavior of a phospholipid extract of a cel$^-$ mutant of *Neurospora crassa.* A phase separation region is observed with onset and completion temperatures of −19 and −6°C, respectively.

INTRODUCTION

Although Raman spectroscopy has been widely applied to the study of phospholipid conformation in model membrane systems (1, 2, and references contained therein), only a few reports dealing with natural membranes or their lipid extracts have appeared (3-6). The main reason for this scarcity of results is the presence of trace fluorescent components in natural systems. Under such conditions, the weak Raman spectrum from the phospholipids is completely lost within the broad fluorescent emission background from the sample. Although there are specific Raman spectroscopic techniques for discriminating against fluorescence (coherent anti-stokes Raman scattering [7], gated detection [8], etc.) being developed, these approaches are likely to be expensive and not generally available in the immediate future.

To extend the applicability of Raman spectroscopy to natural membranes, it was decided to seek a resonance Raman experiment to monitor phospholipid conformation. The advantages of such an approach are: (*a*) Since the resonance Raman signals may be enhanced by factors of 10^4–10^7 from the nonresonance case, the molar intensity of Raman scattering becomes

similar to that of fluorescence. The occurrence of a broad fluorescent background does not then overly complicate the (much sharper) Raman spectrum. (*b*) Whereas other physical techniques require optically homogeneous samples, Raman and resonance Raman spectra are readily obtained from optically inhomogeneous preparations such as membrane films or fragments.

For a chromophore-containing molecule to be useful as a resonance Raman probe of membrane structure, it must satisfy several criteria: (*a*) It must have a strong resonance Raman spectrum. (*b*) The resonance Raman spectrum and therefore the visible absorption spectrum must change in response to conformational changes in the membrane phospholipids. (*c*) The insertion of an external chromophore must not overly perturb the physical properties of the system under investigation. (*d*) The partitioning of the probe molecule into regions of particular order in a membrane must be understood.

Two preliminary resonance Raman studies pertaining to this topic have appeared. Bunow and Levin (9) inserted the channel-forming antibiotic amphotericin B into model membrane systems consisting of dimyristoyl lecithin (DMPC) and DMPC-cholesterol multilayers. In the former, the resonance Raman intensity of the C=C vibrations of the amphotericin B polyene chain was unchanged during the DMPC gel-liquid crystal phase transition. Alterations were noted in the amphotericin spectrum during the broadened phase separation in the DMPC-cholesterol system. The differences in the antibiotic response in the two model systems reflected low penetration of the molecule into the hydrophobic regions of the cholesterol-free system. Amphotericin B is clearly not suited as a general probe of phospholipid order.

Wallach and Verma (10) observed carotenoid bands (particular carotenoid unknown, probably β-carotene) in the Raman spectrum of erythrocyte ghosts and attempted to correlate changes in the relative intensities of the carotenoid bands with alterations in membrane conformation. No detailed analysis of the spectral changes was attempted. In the current study, we have found that power levels similar to those used by Wallach and Verma (3) lead to heating of the sample in the laser beam and eventual destruction of the carotenoid

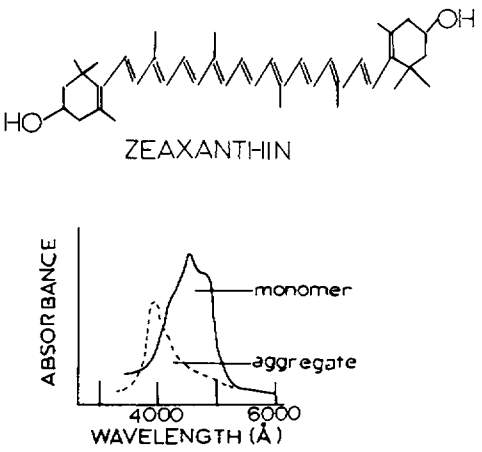

FIGURE 1 Top: Structural formula for zeaxanthin (3R, 3'R)-β,β-carotene-3,3'-diol; bottom: UV-visible absorption spectra of zeaxanthin in acetone (—) and acetone-water (1:9 vol:vol) (----) solutions. The relative intensities are to scale.

moiety. The selection of zeaxanthin ([3R,3R'],β,β-carotene-3-3' diol; structure shown in Fig. 1) as a potential resonance Raman probe was motivated by the following: (*a*) Carey and co-workers (11) and Hager (12) demonstrated large changes in the carotenoid visible absorption spectrum upon addition of water to organic solvent solutions of the molecule. (*b*) Recently, Yamamoto and Bangham (13) showed that similar spectral changes occurred when zeaxanthin was inserted into one component phospholipid suspensions, when the latter were taken through their gel-liquid crystal phase transitions.

In the current work, we demonstrate that zeaxanthin satisfies criteria *a–d* above for a resonance Raman spectroscopic probe reasonably well. The phospholipids chosen to demonstrate this are dipalmitoylphosphatidylcholine (DPPC), distearoylphosphatidylcholine (DSPC), and binary mixtures of the two. The utility of the technique for naturally occurring systems is demonstrated for a phospholipid extract of *Neurospora crassa* cel$^-$ membranes, which contains fluorescent components, is optically inhomogeneous, and has phase transitions below 0°C. It is therefore not easy to study with other physical techniques (such as fluorescence or NMR spectroscopy), and is especially difficult with the ordinary Raman effect.

EXPERIMENTAL

Materials

DSPC and DPPC were obtained from Sigma Chemical Co. (St. Louis, Mo.). Each showed a single spot on highly overloaded TLC plates ($CHCl_3$:MeOH:H_2O,65:25:4) with the appropriate R_f values (14). No further purification was attempted. The phase transition temperatures of the phospholipids as determined from Raman spectroscopic data corresponded to literature values (15). Highly purified zeaxanthin was the generous gift of Dr. G. Saucy, Hoffman-La Roche Inc., Nutley, N.J. Visible absorption data in acetone and acetone-water solution corresponded to literature values (11). The lipid extract from *Neurospora crassa* mutant cel$^-$ was the generous gift of Dr. K. Friedman, New Jersey College of Medicine and Dentistry. The fatty acid composition of the phospholipid hydrocarbon chains is given in Table I. Solvents and reagents were of the highest quality available, and were used without further purification.

Sample Preparations

Stock solutions of zeaxanthin in $CHCl_3$ were stored at 4°C in the dark. Solutions were used for 1 wk only, as significantly longer times led to noticeable sample degradation, presumably due to epoxidation with concomitant loss of visible absorption characteristics.

TABLE I
FATTY ACID COMPOSITION OF THE NEUROSPORA CRASSA (CEL$^-$) MUTANT

Fatty acid Chain length: no. of double bonds	% Total
14:0	0.2
16:0	14.5
16:1	0.6
18:0	1.1
18:1	4.8
18:2	59.0
18:3	19.1
Lignoceric acid	0.6

Samples for spectroscopic study were prepared by adding 0.2 μmol of zeaxanthin in $CHCl_3$ to about 7.6 mg of phospholipid in $CHCl_3$ at the desired DPPC:DSPC mole ratio. The final carotenoid:phospholipid mole ratios were therefore about 1:55. Samples were mixed by vortex action, and solvents were removed by evaporation to dryness. Distilled water was added to the mixture, which was then sonicated with a Heat Systems-Ultrasonics cell disruptor, model W-220 F, equipped with a micro tip (Heat Systems-Ultrasonics, Inc., Plainview, N.Y.). Sonication was carried out above T_m for the phospholipid preparation. Remaining multilamellar material was removed by centrifugation after the sonication. For samples to be used for Raman intensity measurements, $NaClO_4$ was added to a final concentration of 0.6 M. Samples of *Neurospora*/zeaxanthin were prepared from $CHCl_3$ solutions of the components in the manner described above, except that the sonication step was omitted.

Visible Spectroscopy

Visible absorption data were obtained on a Beckman model Acta CIII spectrophotometer equipped with thermostatted cell holders (Beckman Instruments, Inc., Fullerton, Calif.). Samples were contained in matched 1-cm quartz cells. To minimize the effects of light scattering on the background, the reference cuvette always contained the same concentration and mole ratio of phospholipid as in the sample beam, sonicated to the same extent. The concentrations of sonicated zeaxanthin-phospholipid were adjusted so that the absorbance values at λ_{max} were in the range 0.5–1.5. Most of the measured absorbance ratios at a given temperature were obtained from heating runs, in which samples were allowed to equilibrate for 15 min at each temperature. Occasional checks were done in cooling cycles revealed that all spectroscopic changes were reversible, with no signs of hysteresis being observed. Temperature accuracy is estimated at ±0.5°C.

Raman Spectroscopy

Our Raman spectroscopic apparatus has been described previously (16). Zeaxanthin in acetone or acetone-water solution was examined by using rotating cell techniques (17), and 20–30 mW of 4,880-Å excitation from an Ar^+ laser. Phospholipids containing zeaxanthin were injected into melting point capillaries (1 mm i.d.), which were thermostatted in a massive brass block similar to that described by Thomas and Barylski (18). Samples were examined in the transverse mode with only 2–5 mW of laser power for excitation. Power levels of 20 mW led to the gradual loss of intensity of bands arising from the zeaxanthin, indicating that under these conditions, the zeaxanthin was being photochemically altered in the laser beam. For samples of phospholipids free from zeaxanthin, power levels of about 300 mW were used. The Raman intensity of the carotenoid vibrations was compared with that of the symmetric stretching mode of ClO_4^- ion, at 936 cm^{-1}, which was used as an internal standard. Spectra were scanned several times under a given set of conditions and showed carotenoid intensities measurable with a precision of about 5%. Intensities were approximated from peak height measurements. No trend toward sample deterioration was noted except in the case of DSPC/zeaxanthin, where data collected at temperatures above 60°C indicated that carotenoid deterioration took place to a small but measureable extent.

The lipid extract from *Neurospora crassa* (with T_m below 0°C) was examined with the capillary set in an unsilvered glass Dewar flask. Temperature control was achieved by blowing cold nitrogen over the sample and was monitored with a thermistor probe placed in the path of the gas. Temperature accuracy is estimated at ±1°C.

Since internal intensity standards are not reliable for measurements below 0°C for membrane fragments, the phase behavior of the *Neurospora* phospholipid extract was followed by monitoring ν(C═C) of the zeaxanthin. Excellent frequency data (average precision about 0.3 cm^{-1}), could be obtained for this sharp spectral feature, by interpolation of the carotenoid band position between two atomic emission lines from a neon lamp. This procedure was followed for each measurement. Duplicate values were obtained at each temperature.

RESULTS AND DISCUSSION

Zeaxanthin Aggregation in Acetone-Water Mixtures

Visible absorption spectra for zeaxanthin in acetone and acetone/water (1:9 vol:vol) solutions are shown in Fig. 1. The large shift in λ_{max} from 455 to 403 nm that occurs on H_2O addition (Fig. 1) has also been noted by Carey and co-workers (11), who attributed the phenomenon to aggregation of the carotenoid. Their conclusion was based, in part, on measurements of the C=C stretching mode in the zeaxanthin resonance Raman spectrum. It was expected that the large blue shift in λ_{max} would be accompanied by an increase in ν(C=C) in the resonance Raman spectrum consistent with decreased delocalization of the π electron system. However, the blue shift in λ_{max} was accompanied by a 6-cm^{-1} decrease in ν(C=C) from 1,526 to 1,520 cm^{-1}. In addition, Carey et al. were able to collect by centrifugation the species with λ_{max} = 403 nm. It was therefore concluded that carotenoid aggregation occurred on the addition of water, producing the observed visible absorption, resonance Raman, and ultracentrifugation characteristics. According to the description of the aggregation absorption process given by Kasha et al. (19), the blue shift in λ_{max} indicates exciton formation with parallel transition dipoles in the aggregate.

The large changes in the visible absorption spectrum are expected to be accompanied by parallel changes in resonance Raman intensity of the carotenoid (20). To demonstrate this, zeaxanthin aggregation in acetone-water was monitored with resonance Raman spectroscopy. Of interest in the current work are the intense features that appear in all carotenoid spectra at about 1,520 and 1,160 cm^{-1}, which arise from C=C and C—C stretching modes, respectively, in the polyene chain (Fig. 2). The C—C stretching intensity variation was monitored as a function of added water. The nonresonance enhanced acetone vibration near 785 cm^{-1} was used as an internal standard against which the C—C intensity of the carotenoid was compared. Typical results are shown in Fig. 3. The large change in Raman intensity at 40–50% added H_2O is indicative of the onset of aggregation. A shift in the absorption spectrum occurred at the same acetone:water ratio. The Raman intensity from 0–90% added water was decreased by a factor of 150–200. This decrease in intensity is expected since the absorbance of the carotenoid at the wavelength of excitation (4,880 Å) is much lower in the aggregate than in the monomer. The large variation in intensity illustrates the sensitivity of the resonance Raman approach for monitoring changes in a chromophoric system.

Zeaxanthin Aggregation in DPPC, DSPC, and DPPC-DSPC Binary Mixtures

The potential use of zeaxanthin aggregation as a resonance Raman and visible spectroscopic probe of membrane phase behavior was tested in sonicated vesicles of DPPC, DSPC, and binary mixtures of the two. In these experiments, the carotenoid phospholipid mixtures were sonicated to render them optically suitable for absorption spectroscopy. The symmetric stretching mode of the perchlorate ion at 936 cm^{-1} was used as a nonresonance-enhanced internal standard for the Raman intensity measurements. Sodium sulphate was found unsuitable for this purpose, as it induced aggregation of the sonicated vesicles. The resonance Raman spectrum of zeaxanthin inserted into DPPC suspensions is shown in Fig. 2. The data, obtained at 3 mW of laser power, are typical of the worst recorded.

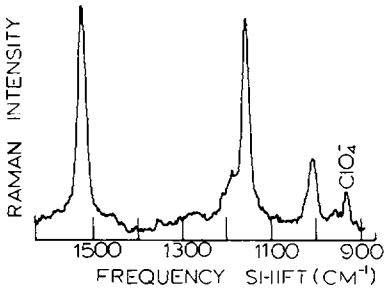

FIGURE 2

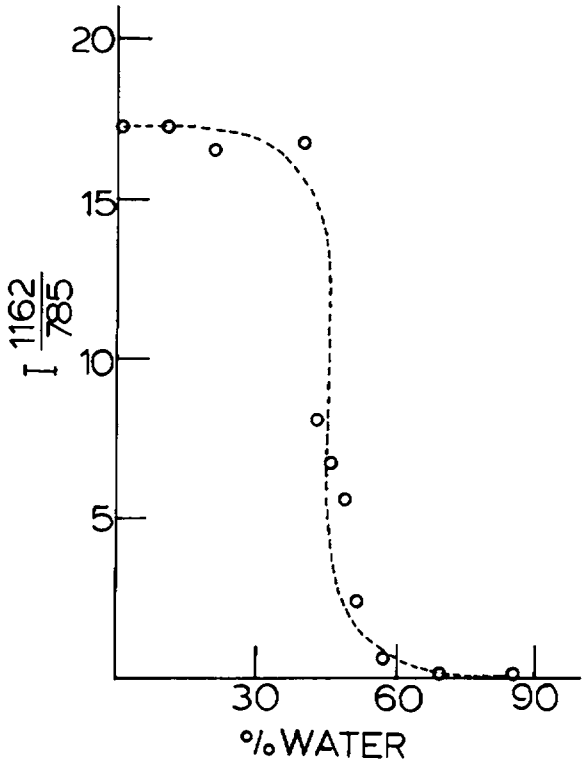

FIGURE 3

FIGURE 2 Typical resonance Raman spectrum of zeaxanthin. The carotenoid was inserted into DPPC multilayers (carotenoid:phospholipid molar ratio 55:1). Spectrum taken at 22°C. Spectral parameters: excitation wavelength 4,880 Å, excitation power ~3 mW, spectral slit width ~6 cm^{-1}, scan speed 0.5 cm^{-1}/s. The C=C peak at 1,521 cm^{-1} has an intensity corresponding to about 3,000 cps. The band at 936 cm^{-1} arises from ClO_4^- which was present as $NaClO_4$ at 0.6 M. Spectra of zeaxanthin in acetone/H_2O solution had peak signal:noise ratios significantly better than the spectrum shown here.

FIGURE 3 Variation of zeaxanthin C—C resonance Raman intensity as a function of added water in acetone-water solution. The acetone band at 785 cm^{-1} was used as an internal standard. The zeaxanthin:acetone mole ratio is constant. Spectra were obtained in a rotating cell by using 4,880-Å excitation.

The absorption spectral data for zeaxanthin in sonicated DPPC is dependent on the phospholipid:carotenoid molar ratio in the vesicles. This phenomenon is illustrated in Fig. 4. At 7:1 mole ratio (22°C), λ_{max} appears at 407 nm, close to the position observed by Yamamoto and Bangham for zeaxanthin in multilamellar liposomes at 25:1 mole ratio (13). When the phospholipid:carotenoid ratio is increased to 50:1 the absorption spectrum is red-shifted with λ_{max} at 430 nm. Above T_m for DPPC, a further shift in the absorption spectrum is noted, with the resultant spectrum resembling that of the monomer of zeaxanthin in acetone solution, except for the loss of some fine structure (compare Fig. 4 with Fig. 1). The concentration-dependent shift in λ_{max} below T_m is not observed for DSPC at these concentration levels. The carotenoid spectrum in gel state DSPC (50:1 molar ratio) has λ_{max} near 407 nm. The similarities in the absorption and resonance Raman data (see below) of zeaxanthin in

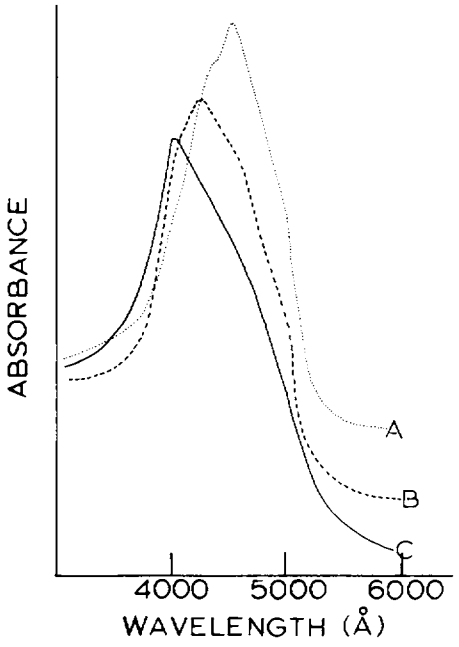

FIGURE 4

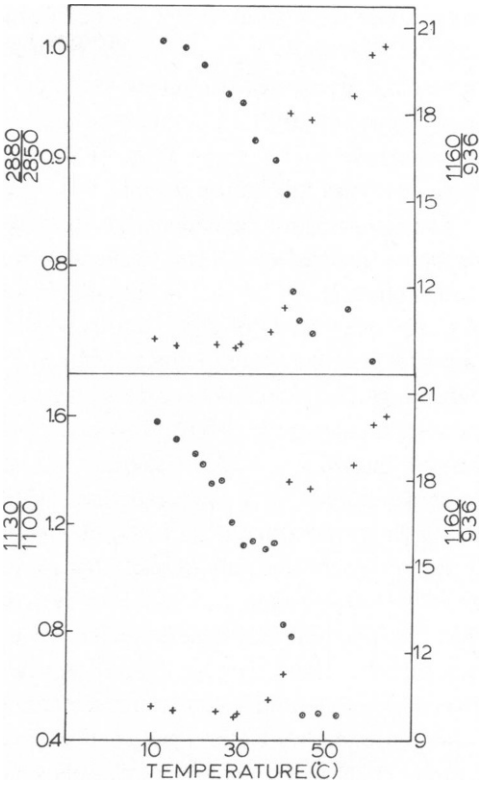

FIGURE 5

FIGURE 4 Absorption spectra of zeaxanthin inserted into DPPC vesicles under the following conditions: (*A*) DPL:zeaxanthin 55:1 mole ratio T = 60°C; λ_{max} = 455 nm. (*B*) DPL:zeaxanthin 55:1 mole ratio T = 22°C; λ_{max} = 430 nm. (*C*) DPL:zeaxanthin 7:1 mole ratio T = 22°C; λ_{max} = 407 nm. Spectra have been displaced for clarity along the vertical axis.

FIGURE 5 Top: Temperature-induced variation in I 1,160:936 for zeaxanthin in sonicated vesicles of DPPC (+, right-hand scale) and for the nonresonant enhanced parameter I 2,880:2,850 for DPPC sonicated vesicles without zeaxanthin (O, left-hand scale). Bottom: Temperature-induced variation in I 1,160:936 for zeaxanthin in sonicated DPPC vesicles (+, right-hand scale) and for the nonresonant enhanced parameter I 1,130:I 1,100 for sonicated DPPC vesicles without zeaxanthin (O, left-hand scale). The I 1,130:1,100 ratio can be directly related to the number of gauche rotamers in the phospholipid hydrocarbon chains.

acetone-water solutions and in phospholipid suspensions, lead us to suggest that the carotenoid molecule responds to changes in phospholipid hydrocarbon chain order, by undergoing an aggregation-disaggregation process in the model membrane similar to the one occurring in acetone-water solution. This interpretation does not require the invoking of a conformational change in the zeaxanthin, as has been previously suggested (13).

If the above interpretation is correct, the origin of the concentration dependent shift in the zeaxanthin-containing DPPC may be related to the imperfect packing of the phospholipid hydrocarbon chains in the small vesicle preparations used in the current work (2). The extensive noncooperative formation of gauche rotamers below T_m in such systems (2) may

cause some carotenoid at low concentrations to partition into disordered regions of DPPC vesicles. This shifts λ_{max}, so that the resultant absorption spectrum is a linear combination of remaining aggregated carotenoid spectrum plus spectrum of monomer that has formed in the fluid regions of DPPC. Computer simulations involving additions of the absorption spectra of the monomer and the aggregate (R. Mendelsohn and W. Castner, unpublished work) are consistent with this interpretation.

The temperature dependence of the resonance Raman intensity for zeaxanthin in DPPC vesicles measured by *I* 1160:936 is shown in Fig. 5. A clear melting region is noted with a transition range of 38–42° in reasonable agreement with that measured by other techniques (2). The magnitude of the intensity variation in the resonance Raman spectrum is only a factor of 2 as compared with a factor of 150–200 observed for the carotenoid aggregation-disaggregation in acetone-water solution. This difference is attributed to the formation of carotenoid monomer in DPPC vesicles below T_m alluded to previously. Since most of the Raman intensity at 4880-Å excitation is derived from zeaxanthin monomer, the factor of 2 intensity increase at T_m suggests that about 50% of the carotenoid is in monomer form below the onset temperature at 50:1 phospholipid:carotenoid ratios. The factor of 150–200 variation in the resonance Raman intensity for zeaxanthin aggregation in acetone-water suggests that at 90% H_2O the aggregation is (nearly) complete. To verify that the insertion of zeaxanthin into phospholipid suspensions under the conditions of the experiment does not extensively perturb the DPPC phase transition, the resonance Raman intensity data for DPPC-zeaxanthin was compared to nonresonance Raman data for sonicated DPPC vesicles in Fig. 5. Two nonresonance Raman parameters have been widely used to characterize DPPC melting (2,22). Hydrocarbon chains of the phospholipid give rise to strong conformation-dependent Raman bands. The C—C stretching mode at 1,130 cm^{-1} is associated with chains in the all-*trans* conformation, while the feature at 1,100 cm^{-1} is derived from hydrocarbon chains containing gauche rotations. The *I* 1,130:1,100 intensity ratio quantitively measures the number of phospholipid hydrocarbon chain segments in the all-*trans* conformation (2). The 2,880:2,850 intensity ratio, derived from chain C-H stretching modes, responds to changes in both the lateral packing of the chains and the *trans*-gauche population ratio. The temperature-induced changes in these spectral regions for the DPPC vesicles used in the current work are shown in Fig. 5. They have been discussed elsewhere in detail (2, 23). The 1,130:1,100 ratio shows a rapid variation at the main transition centered at 41°C. The trend of the data in the 30–35° range is consistent with a small fraction of the vesicles undergoing a premelting process. Since sonicated preparations normally do not undergo pretransitions (24), it is possible that aggregation occurred to a slight extent during the time (8 h) required for a melting curve determination by Raman spectroscopy. Also seen is the noncooperative formation of gauche rotamers between 10–30°C as indicated by variation in the intensity parameter from 1.6 to 1.1. The resonance Raman data for zeaxanthin in DPPC are compared with nonresonance data in Fig. 5. The similarities in the onset and completion temperatures for the main transition as measured by zeaxanthin aggregation-disaggregation (resonance Raman) or by direct observation of gauche rotamer formation (*I* 1,130:1,100) suggests that there is no extensive perturbation of phospholipid phase behavior by the carotenoid molecule. However, the resonance Raman parameter does not respond to the noncooperative formation of gauche rotamers below T_m, as *I* 1,160:936 is constant between 10° and 30°C. Zeaxanthin

either inhibits the noncooperative formation of gauche rotamers or requires cooperative gauche rotamer formation to undergo further monomer formation. Using turbidity measurements on multilamellar liposomes, Yamamoto and Bangham (13) have seen a slight perturbation in the DPPC melting profile in 25:1 phospholipid:zeaxanthin mole ratio preparations. The effect was greatest in the premelt region which is (nearly) abolished in the current work by the sonication procedures. Resonance Raman data for zeaxanthin in DSPC vesicles exhibit onset and completion temperatures of 50 ± 2°C and 54 ± 2°C, respectively, as measured by the 1,160:936 intensity ratio.

The phase transitions in DPPC and DSPC have also been monitored using visible absorption data, and the results are shown in Fig. 6. The phase transitions in DSPC and DPPC were monitored via alterations in the 455:407- and 455:430-nm intensity ratios, respectively. Different parameters were used in each instance because the formation of zeaxanthin monomer in DPPC leads to λ_{max} at 430 nm, as previously discussed. The onset and completion temperatures, as measured by visible spectroscopy, are in good agreement with the resonance Raman data. In addition, melting curves for DPPC containing zeaxanthin in a 12:1 phospholipid:carotenoid mole ratio were constructed by using the 455:407-nm intensity ratio as a probe. Onset and completion temperatures were the same as for the 55:1 DPPC:zeaxanthin system measured by using I 455:430. These data suggest that the carotenoid levels used here do not perturb the phase characteristics of the phospholipids, and furthermore that the perchlorate ion used as an internal intensity standard in the resonance Raman experiments

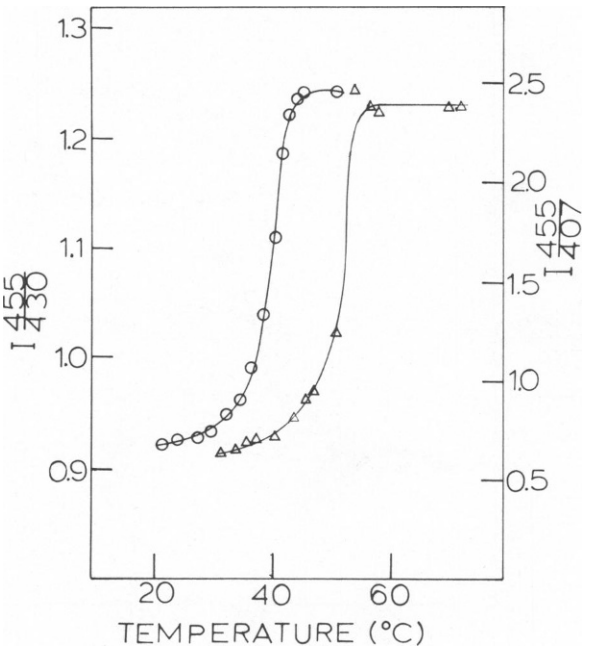

FIGURE 6 The temperature-induced change in the visible absorption spectrum of zeaxanthin in DPPC (o) and DSPC (Δ) sonicated vesicles as measured by the 455:430- and 455:407-nm intensity ratios, respectively. See text for discussion of different parameters used to characterize the melting.

does not affect the melting profiles in one-component phospholipid systems, as the results in Fig. 6 were obtained for samples lacking perchlorate.

Before using this method for phase transition studies in natural membranes and their lipid extracts, it is necessary to test the method in model systems that possess phase properties resembling those in vivo. Phase transitions (separations) in bacterial membranes and their lipid extracts are broadened from the essentially first-order characteristics observed in one-component systems, as expected from thermodynamic considerations (25). The membranes are viable only in temperature regions where the gel and liquid crystal phases coexist; i.e., at temperatures "within" the phase separation region. The simplest phospholipid systems can mimic the phase behavior of bacterial membranes are binary mixtures. Phase diagrams for the latter have been reported by several groups using diverse approaches such as ESR (26, 27), differential scanning calorimetry (15, 28, 29) and fluorescence (30, 31). The DPPC-DSPC system chosen in the current work to test the zeaxanthin aggregation has been studied by Shimshick and McConnell (26), who used as a probe partitioning of a 2,2,6,6-tetramethylpiperidine-1-oxyl (TEMPO) spin label into fluid regions of the mixture. The phase diagram constructed from visible or resonance Raman data in the current work can be compared directly with the earlier studies to evaluate the perturbations caused by the probe molecule.

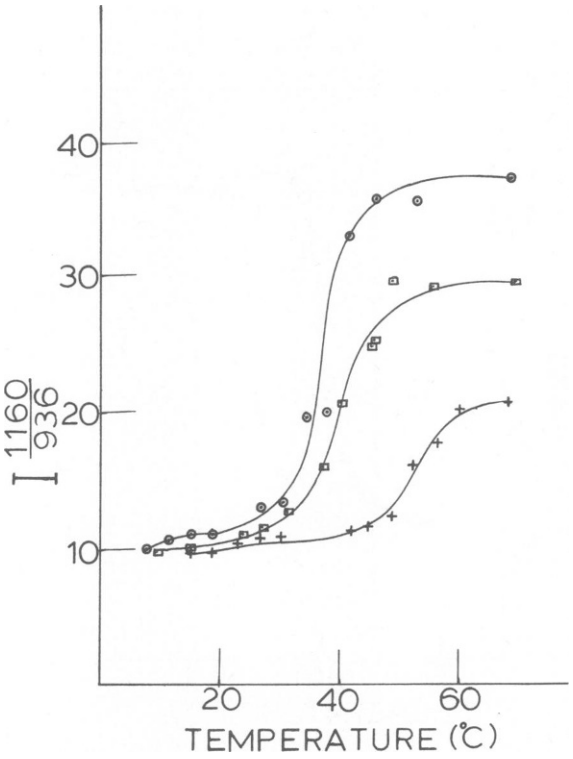

FIGURE 7 Temperature-induced variation in the resonance Raman spectrum as measured by I 1,160:936 for zeaxanthin inserted into the following DPPC:DSPC mixtures: o, 3:1 (wt:wt) DPPC:DSPC; □, 1:1 (wt:wt) DPPC:DSPC; and +, 1:3 (wt:wt) DPPC:DSPC.

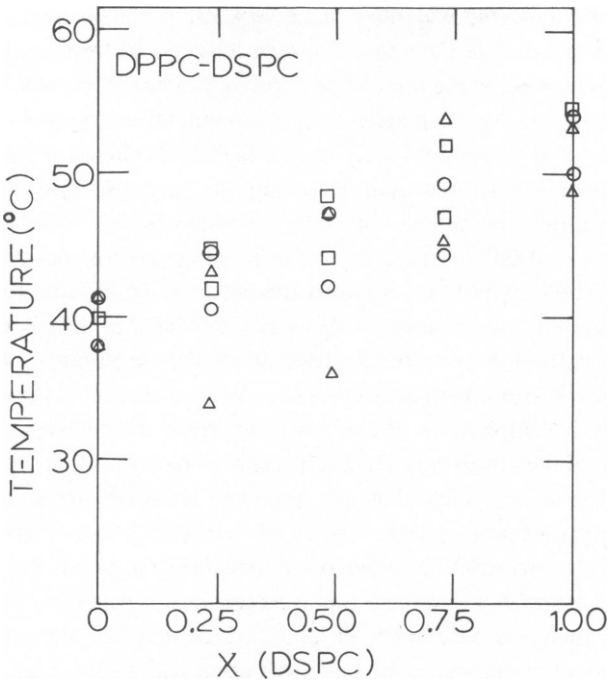

FIGURE 8 Phase diagram for DPPC/DSPC binary system measured 3 different ways: ○, visible absorption data (current work); △, resonance Raman data (current work); and □, data points obtained from ESR data of Shimshick and McConnell (6). The ESR data were for multilamellar vesicles; the visible and resonance Raman data were for sonicated (mostly unilamellar) vesicles.

Melting curves derived from resonance Raman intensity data at several DPPC:DSPC concentrations are shown in Fig. 7. The onset and completion temperatures were estimated from each curve by extrapolation of the linear portions. The region of phase separation in each instance is broadened from the 4° range observed for the one-component cases. The data points for phase diagram construction are plotted in Fig. 8. Also shown are data obtained in the current work from visible absorption spectroscopic measurements and the data points of Shimshick and McConnell obtained from ESR studies (26).

The ESR and visible absorption data for the binary systems are in reasonable agreement, the average deviations between the two approaches in general being 1½–2°. These discrepancies, along with the broadened melting regions of the one-component systems as measured from absorption spectroscopy, can be explained on the basis that sonicated samples were used in the current study while multilamellar vesicles were used in the ESR experiments. In addition, the TEMPO spin label method may itself suffer from inaccuracies.

The completion temperatures as determined from the resonance Raman spectroscopic data (Fig. 8) agree with the other approaches. However, the onset temperatures for phase separation in the samples with 33 and 50 wt % DSPC are reduced by ~4° from the other two approaches. The explanation for this is unclear. It is unlikely that local heating in the sample caused by the laser (which would produce a low onset temperature) is responsible since very low power levels were used, and not all samples showed the problem. It is possible that the high levels of $NaClO_4$ (0.6 M) could affect certain regions of the phase diagram in the binary

mixture. These as yet unexplained deviations between the resonance Raman and other approaches limit the accuracy of the phase diagram constructed from intensity data.

A question of importance for the use of this approach to monitor phase behavior in natural membranes is the quantitative estimation of the amount of carotenoid that partitions into either gel or liquid crystal phase lipid in systems where both phases are present. An attempt was made to directly measure this quantity along the lines used by Sklar et al. (31) for parinaric acid. Zeaxanthin was mixed with DPPC vesicles (45°C, liquid liquid crystal state) and allowed to mix with DSPC vesicles at the same temperature (gel phase). It was hoped that the carotenoid would equilibrate between the gel state DSPC and the liquid crystalline DPPC. These experiments were unsuccessful (as were ones in which the carotenoid was inserted into DSPC initially), presumably because of the insolubility of the carotenoid in water, which inhibits the attainment of equilibrium. We are currently addressing this question of partitioning using a combination of the phase diagram of the binary lipid mixture and computer simulation of the absorption spectra in the region of phase separation. It is clear that the partition coefficients are such that the presence of small amounts of one phase of phospholipid in the presence of a large excess of a second phase is insufficient to induce complete transfer of the carotenoid into the lower concentration phase. For example, if a trace of liquid crystal phospholipid induced the zeaxanthin to partition (in monomer form) completely into it, then measurements of phase transitions would sense only the onset temperatures and would always have the same transition width. Since the observed transition widths are quite broad and variable (4–8°C), the carotenoid must not exclusively partition into either ordered or disordered phospholipid phases when both are present.

It appears that zeaxanthin satisfies the four criteria set out earlier for a resonance Raman probe subject to the following limitations:

(*a*) Occasional low onset temperatures limit the accuracy in determination of the midpoint of the transition. The origin of the uncertainty may be resolved in future studies. (*b*) In natural systems, it is not clear how the presence of protein will affect the zeaxanthin aggregation mechanism. Thus a variety of experiments at various lipid:protein ratios are necessary to calibrate the method in 3-component systems.

Zeaxanthin Aggregation in a Lipid Extract from Neurospora crassa Membranes

As an initial demonstration of utility of this method for monitoring phase properties of natural membranes, carotenoid aggregation has been studied in phospholipids extracted from a *Neurospora crassa* cel$^-$ mutant. Zeaxanthin was added to the lipid extract in a phospholipid:carotenoid molar ratio of 55:1. Since it was expected that T_m for this system was below 0°C, an approach to the resonance Raman experiment different from the measurement of intensity variation used previously had to be adopted. (It is difficult to find a suitable Raman internal intensity standard for a membrane suspension in which the temperature has to be taken through 0°C.) As an alternative approach, we have monitored the variation in the zeaxanthin C═C stretching frequency that was found by Carey et al. (11) (and confirmed by us) to vary from 1,526 cm^{-1} in the monomer to 1,520 cm^{-1} in the aggregate. To obtain reproducible measurements so that this small variation in νC═C could be used to construct a melting curve, the procedure as described in the Experimental section had to be followed rigorously. The melting profile for the lipid extract is shown in Fig. 9. This sigmoid shaped

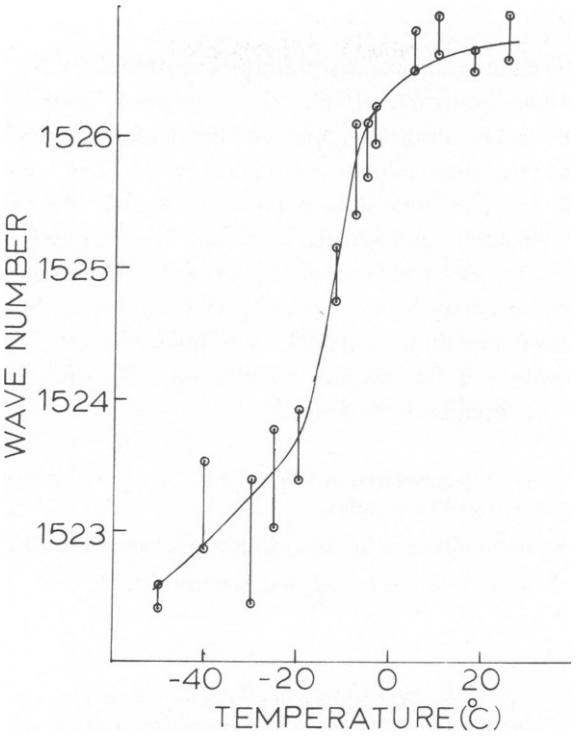

FIGURE 9 Temperature-induced variation in $\nu_{C=C}$ for zeaxanthin inserted into multilayers of a *Neurospora crassa* (cel$^-$ mutant) lipid extract. Phospholipid:carotenoid mole ratio was 55:1. Average precision in frequency data was about 0.3 cm^{-1}. See text for details.

curve has onset and completion temperatures of -19 and -6°C, respectively, with a midpoint at -13°C. The data are in good agreement with calorimetric studies of the same system.[1] It is clear from the fatty acid composition (Table I) that the 18:2 chain is dominant. The phase transition for this hydrocarbon (although head group dependent) is expected to be below 0°C, as observed here.

An advantage of the frequency measurement for studying the phase transition is that optically homogeneous samples are not required. Although the magnitude of the frequency shift during a transition is only 3–4 cm^{-1} (Fig. 9), it is possible to monitor this change with a precision of 0.3–0.5 cm^{-1}, so that useful melting curves can be obtained. Current studies are focused on finding a suitable internal standard for Raman intensity measurements in optically opaque systems. These would be useful since the intensity change during a transition is about a factor of 2–4 (Fig. 7), and can be measured with a precision of 5%. Thus the precision in the intensity measurement would be significantly better than in a frequency measurement. On the other hand, the frequency measurement does not suffer from the possible perturbations that may arise from the high concentration of internal standard necessary for the intensity measurement.

[1]Friedman, K. Private communication.

CONCLUSIONS

(*a*) The aggregation/disaggregation of zeaxanthin is controlled by the conformation of the phospholipid hydrocarbon chains into which the carotenoid is inserted. The large changes produced in both the visible absorption and the resonance Raman spectra permit this phenomenon to be used as a phospholipid structure probe. (*b*) The presence of carotenoid at the levels used in the current work does not overly perturb the phase behavior of the phospholipids. (*c*) Fluorescent components need not be rigorously excluded from the membrane preparations to obtain resonance Raman data. Thus the scope of the current approach is broader than ordinary Raman measurements, and can be extended to encompass a wide variety of natural membranes and/or their lipid extracts. The resonance Raman approach, unlike absorption or fluorescence spectroscopy, can sample optically inhomogeneous preparations such as membrane fragments.

We thank Dr. K. Friedman for generously supplying us with the *Neurospora crassa* lipid extract, and Dr. G. Saucy of Hoffmann-La Roche for supplying us with zeaxanthin.

We thank the Busch Memorial Fund of Rutgers University for partial support of this work (to Dr. Mendelsohn).

Received for publication 3 January 1979 and in revised form 19 March 1979.

REFERENCES

1. YELLIN, N., and I. W. LEVIN. 1977. Hydrocarbon chain disorder in lipid bilayers. Temperature dependent Raman spectra of 1–2 diacylphosphalidylcholine water gels. *Biochim. Biophys. Acta.* **489**:177–190.
2. GABER, B. P., and W. L. PETICOLAS. 1977. On the quantitative interpretation of biomembrane structure by Raman spectroscopy. *Biochim. Biophys. Acta.* **465**:260–274.
3. VERMA, S. P., and D. F. H. WALLACH. 1976. Erythrocyte membranes undergo cooperative, pH-sensitive state transitions in the physiological temperature range: Evidence from Raman spectroscopy. *Proc. Natl. Acad. Sci. U.S.A.* **73**:3558–3561.
4. MILANOVICH, F. P., B. SHORE, R. C. HARNEY, and A. T. TU. 1976. Raman spectroscopic analysis of dutch belt rabbit erythrocyte ghosts. *Chem. Phys. Lipids.* **17**:79–84.
5. LIPPERT, J. L., L. E. GORZYCA, and G. MEIKLEJOHN. 1975. A laser Raman spectroscopic investigation of phospholipid and protein configurations in hemoglobinfree erythrocyte ghosts. *Biochim. Biophys. Acta.* **382**:51–57.
6. ROTHCHILD, K. S., J. R. ANDREW, W. J. DEGRIP, and H. E. STANLEY. 1976. Opsin structure probed by Raman spectroscopy of photoreceptor membranes. *Science (Wash. D. C.).* **191**:1176–1178.
7. NIBLER, J. W., W. M. SHAUB, J. R. MCDONALD, and A. B. HARVEY. Coherent antistokes Raman scattering. *In* Vibrational Spectra and Structure. J. R. Durig, editor. Elsevier Scientific Publishing Co., New York. Vol. 6. 1977.
8. VAN DUYNE, R. P., D. L. JEANMAIRE, and D. F. SHRIVER. 1974. Mode-locked laser Raman spectroscopy: A new technique for the rejection of interfering background luminescence signals. *Anal. Chem.* **46**:213–222.
9. BUNOW, M. R., and I. W. LEVIN. 1977. Vibrational Raman spectra of lipid systems containing amphotericin B. *Biochim. Biophys. Acta.* **464**:202–216.
10. WALLACH, D. F. H., and S. P. VERMA. 1975. Raman and resonance-Raman scattering by erythrocyte ghosts. *Biochim. Biophys. Acta.* **382**:542–441.
11. SALARES, V. R., N. M. YOUNG, P. R. CAREY, and H. J. BERNSTEIN. 1977. Excited state (exciton) interactions in polyene aggregates. *J. Raman Spectrosc.* **6**:282–288.
12. HAGER, A. 1970. Formation of maxima in the absorption spectrum of carotenoids in the region around 370 nm; Consequences for the interpretation of certain action spectra. *Planta (Berl.).* **91**:38–53.
13. YAMAMOTO, H. Y., and A. D. BANGHAM. 1978. Carotenoid organization in membranes. Thermal transition and spectral properties of carotenoid containing liposomes. *Biochim. Biophys. Acta.* **507**:119–127.
14. KATES, M. 1972. Techniques of Lipidology. T. S. Work and E. Work, general editors. North Holland Publishing Co., Amsterdam. 269–610.

15. MABREY, S., and J. M. STURTEVANT. 1976. Investigation of phase transitions of lipids and lipid mixtures by high sensitivity differential scanning calorimetry. *Proc. Natl. Acad. Sci. U.S.A.* **73**:3862–3866.
16. MENDELSOHN, R., and J. MAISANO. Use of deuterated phospholipids in Raman spectroscopic studies of membrane structure. Multilayers of dimyristoyl phospholidylcholine (and its $-d_{54}$ derivative) with distearoyl phosphatidylcholine. *Biochim. Biophys. Acta.* **506**:192–201.
17. KIEFER, W., and H. J. BERNSTEIN. A cell for resonance Raman excitation with lasers in liquids. *Appl. Spectrosc.* **25**:500–501.
18. THOMAS, G. J., Jr., and J. R. BARYLSKI. 1970. Thermostatting capillary cells for a laser-Raman spectrophotometer. *Appl. Spectrosc.* **24**:463–464.
19. KASHA, M., H. R. RAWLS, and M. ASHRAF EL-BARJOUMI. 1965. The exciton model in molecular spectroscopy. *Pure Appl. Chem.* **11**:371–392.
20. INAGAKI, F., M. TASUMI, and T. MIYAZAWA. 1974. Excitation profile of the resonance Raman effect of β-carotene. *J. Mol. Spectrosc.* **50**:286–303.
21. RIMAI, L., M. E. HEYDE, and D. GILL. 1973. Vibrational spectra of some carotenoids and related linear polyenes. A Raman spectroscopic study. *J. Am. Chem. Soc.* **95**:4493–4501.
22. MENDELSOHN, R., and T. TARASCHI. 1978. Deuterated phospholipids as Raman spectroscopic probes of membrane structure: Dipalmitoylphosphatidylcholine-dipalmitoylphospholidylethanolamine multilayers. *Biochemistry.* **17, 19**:3944–3949.
23. MENDELSOHN, R., S. SUNDER, and H. J. BERNSTEIN. 1976. The effect of sonication on the hydrocarbon chain conformation in model membrane systems: A Raman spectroscopic study. *Biochim. Biophys. Acta.* **419**:563–569.
24. SUURKUUSK, J., B. R. LENTZ, Y. BARENHOLZ, R. L. BILTONEN, and T. E. THOMPSON. 1976. A calorimetric and fluorescent probe study of the gel-liquid crystalline phase transition in small, single-lamellar dipalmitoylphosphatidylcholine vesicles. *Biochemistry.* **15**:1393–1401.
25. LEE, A. G. 1977. Lipid phase transitions and phase diagrams II. Mixtures involving lipids. *Biochim. Biophys. Acta.* **472**:285–344.
26. SHIMSHICK, E. J., and H. M. MCCONNELL. 1973. Lateral phase separation in phospholipid membranes. *Biochemistry.* **12**:2351–2360.
27. LUNA, E. J., and H. M. MCCONNELL. 1977. Lateral phase separations in binary mixtures of phospholipids having different charges and different crystalline structures. *Biochim. Biophys. Acta.* **470**:303–316.
28. BLUME, A., and T. ACKERMANN. 1974. A calorimetric study of the lipid phase transitions in aqueous dispersions of phosphorylcholine-phosphorylethanolomine mixtures. *F.E.B.S. (Fed. Eur. Biochem. Soc.) Lett.* **43**:71–74.
29. CHAPMAN, D., J. URBINA, and K. M. KEOUGH. 1974. Biomembrane phase transitions. Studies of lipid-water systems using differential scanning calorimetry. *J. Biol. Chem.* **249**:2512–2521.
30. SKLAR, L. A., B. S. HUDSON, M. PETERSEN, and J. DIAMOND. 1977. Conjugated polyene fatty acids as fluorescent probes: Spectroscopic characterization. *Biochemistry.* **16**:813–818.
31. SKLAR, L. A., B. S. HUDSON, and R. D. SIMONI. 1977. Conjugated polyene fatty acids as fluorescent probes: Synthetic phospholipid membrane studies. *Biochemistry.* **16**:819–828.